Title

Synthesis of Polyisobutylene Bottlebrush Polymers via Ring-Opening Metathesis Polymerization

Journal

Macromolecules, 50(19)

ISSN

0024-9297

Authors

Yang, Bin
Abel, Brooks A
McCormick, Charles L
et al.

Publication Date

2017-10-10

DOI

10.1021/acs.macromol.7b01655

Peer reviewed

Macromolecules

Article

pubs.acs.org/Macromolecules

Synthesis of Polyisobutylene Bottlebrush Polymers via Ring-Opening Metathesis Polymerization

Bin Yang, Brooks A. Abel, Charles L. McCormick, and Robson F. Storey*

School of Polymer Science and Engineering, The University of Southern Mississippi, 118 College Dr. # 5050, Hattiesburg, Mississippi 39406, United States

Supporting Information

ABSTRACT: Polyisobutylene (PIB)-based bottlebrush polymers were synthesized via ring-opening metathesis polymerization (ROMP) of norbornene- and oxanorbornene-terminated PIB macromonomers (MM) initiated by Grubbs third-generation catalyst ($(H_2IMes_2)(pyr)_2(Cl)_2Ru{=}CHPh$) (G3). While both MMs reached greater than 97% conversion as measured by ^1H NMR, the rate of propagation of PIB norbornene was measured to be 2.9 times greater than that of PIB oxanorbornene MMs of similar molecular weight (MW). The slower rate of propagation of the oxanorbornene MM was attributed to interaction between the electron-rich oxygen bridge and the metal center of G3, which slowed but did not inhibit polymerization. Both types of MMs demonstrated controlled/"living" polymerization behavior, and brush polymers with MWs up to ~700 kg/mol with narrow dispersity ($Đ \leq 1.04$) were achieved.

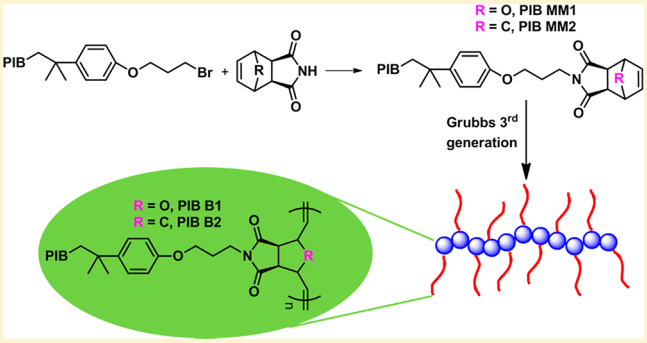

INTRODUCTION

Bottlebrush polymers are of great interest owing to their highly branched polymer topology, well-defined and tailorable dimensions, and unique mechanical and rheological properties.[1] Bottlebrush polymers consist of macromolecular side chains covalently attached to a polymer backbone and exhibit a chain extended conformation caused by the steric repulsions between crowded neighboring side chains.[2] The morphology of bottlebrush polymers can be tailored by controlling polymer composition, graft density, and/or side chain length to achieve cylindrical,[3,4] spherical,[5,6] or wormlike morphologies.[1] Through proper selection of polymeric side chains, essential properties including stimuli-responsiveness[1,7] and amphiphilicity,[8,9] can be incorporated into the bottlebrush polymers. Unlike most linear, flexible-chain polymers, bottlebrush polymers lack significant chain entanglement due to steric repulsion of polymeric side chains, resulting in relatively low viscosity even at very high MW.[10,11]

In general, there are three basic methods of preparing bottlebrush polymers,[12−15] termed "grafting-from",[16,17] "grafting-onto",[18−20] and "grafting-through".[21−23] Of these techniques, the grafting-through strategy is the most versatile route and involves first preparation of macromonomers (MM) with polymerizable end-functional groups, followed by controlled/"living" polymerization to form bottlebrush polymers.[21−23] "Grafting-through" affords precise control over the backbone and side chain length, while ensuring 100% grafting density since the polymerizeable moiety is inherently bound to each side chain. However, it remains difficult to achieve brush polymers with high degrees of polymerization (DP) and low dispersities, largely due to the steric hindrance associated with polymerizing macromonomers.

Lately, numerous examples of bottlebrush polymer syntheses with near-quantitative MM conversion and narrow dispersities have been reported via ROMP using ruthenium-based metathesis catalysts, owing to their fast initiation, high activities, and excellent functional group tolerance.[11−13,15,24−35] However, despite the recent developments regarding brush polymer synthesis via ROMP, synthesis of norbornene end-functional MMs still remains a challenge. The two primary approaches used to synthesize norbornene-functional MMs are "direct-growth" (DG-MM) and "growth-then-coupling" (GC-MM).[31] The DG-MM approach involves the use of a norbornene-functional initiator or chain transfer agent to afford norbornene-functional MMs.[13,15,30,36−38] However, there are several concerns regarding the DG-MM approach. Copolymerization or other reaction of the norbornene olefin during polymerization must be minimized.[39] Furthermore, small traces of difunctional norbornene MMs arising from bimolecular coupling during radical polymerization generally lead to undesired brush branching and increased polydispersity of the resulting brushes.[31] Alternatively, the GC-MM strategy involves creation of a MM precursor in the absence of the norbornene moiety, followed by postpolymerization end-group functional-

Received: August 1, 2017
Revised: September 8, 2017
Published: September 19, 2017

DOI: 10.1021/acs.macromol.7b01655
Macromolecules 2017, 50, 7458−7467

Scheme 1. Synthesis of PIB (Oxa)norborene MMs and Their Corresponding Bottlebrush Polymers via ROMP

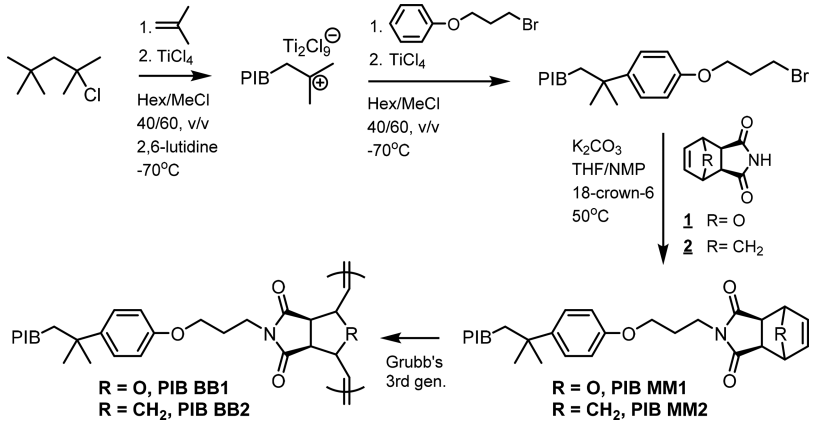

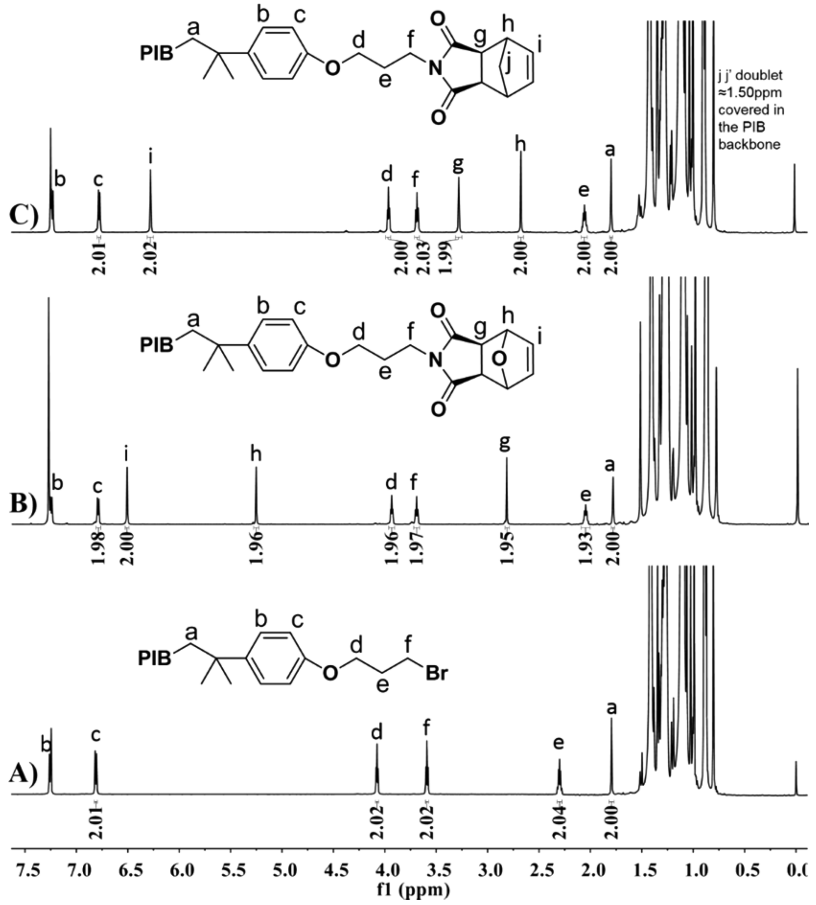

Figure 1. ^{1}H NMR spectra (600 MHz, 25 °C, $CDCl_3$) of monofunctional (A) PIB Br, (B) PIB oxanorbornene, and (C) PIB norbornene MM.

ization ("coupling") to produce the desired norbornene-functional macromonomer.

Most ROMP MMs have been prepared using living polymerization techniques, especially radical and anionic polymerizations, to achieve precisely MWs and near-quantitative end-group functionality.[40−42] However, to the best of our knowledge, there have been no reports on the preparation of ROMP MMs by living carbocationic polymerization (LCP), and in particular, we are unaware of any reports on the synthesis of norbornene-functional polyisobutylene (PIB)-based MMs. In fact, the only literature reports regarding PIB and ROMP pertain to ruthenium catalyst recycling by binding PIB to the *N*-heterocyclic carbene ligand of Grubbs II catalyst.[43] Recently, the synthesis of PIB brush polymers has been reported by RAFT polymerization of PIB acrylate MMs.[44] However, this approach required long reaction times (>24 h) and high initiator concentrations to achieve high conversion. Furthermore, the polydispersity ($Đ$) of obtained PIB brushes was greater than 2.0.

PIB is an excellent candidate for introduction into bottlebrush polymers because of its unique properties, including high flexibility and energy damping, good thermal and oxidative stability, low gas permeability, good chemical and solvent resistance, and good biocompatibility.[45] Moreover, with

DOI: 10.1021/acs.macromol.7b01655
Macromolecules 2017, 50, 7458−7467

only several exceptions,[6,46] there have been very few literature reports of bottlebrush polymers composed of polyolefin side chains. With the development of LCP of PIB, a broad family of PIB MMs has been reported, such as (meth)acrylates[47−49] and epoxides.[50] Recent work in chain-end functionalization of PIB offers promising new routes for facile synthesis of functionalized PIBs with quantitative end-group conversion, precisely controlled MWs, and narrow $Đ$.[51−54]

In this paper, we report the synthesis of norbornene-functional PIB MMs and their incorporation into bottlebrush polymers using ROMP. We used a GC-MM synthetic route, in part because norbornene olefins are known to undergo carbocationic rearrangement polymerization.[55] As shown in Scheme 1, we used nucleophilic substitution of PIB-Br with *exo*-(oxa)norbornene dicarboximides, **1** and **2**, followed by ROMP initiated from Grubb's III (G3) catalyst to produce various high MW brush polymers with controlled MW and narrow $Đ$ (Scheme 1). We also report the effect of norbornene bridge group on the ROMP kinetics of PIB norbornene and PIB oxanorborne MMs initiated by G3 catalyst as measured by both ^{1}H NMR and SEC kinetic analyses.

RESULTS AND DISCUSSION

Synthesis of PIB Oxanorbornene (PIB MM1) and PIB Norbornene (PIB MM2) Macromonomers. The two *exo*-(oxa)norbornene dicarboximide precursors (**1** and **2**) were synthesized as shown in Scheme S1 (Supporting Information). While *exo*-norbornene dicarboximide derivatives such as **2** typically exhibit higher rates of polymerization by ROMP as compared to their *exo*-oxanorbornene analogues,[56] the high yield and single-step synthesis of *exo*-oxanorbornene dicarboximide **1** warranted the investigation of its use in preparing PIB-based MMs. The structures of both norbornene precursors were confirmed by ^{1}H NMR (Figure S1) and ^{13}C NMR (Figure S2).

PIB-Br was prepared by end-quenching of living carbocationic PIB at full IB monomer conversion with (3-bromopropoxy)benzene. PIB (oxa)norbornene macromonomers were then synthesized by nucleophilic substitution reaction of PIB-Br with precursors **1** and **2**.[57] A mild reaction temperature of 50 °C was adopted to prevent decomposition of the (oxa)norbornene moiety via retro-Diels−Alder reaction.[58]

Structural Characterization of PIB (Oxa)norbornene Macromonomers. The structures of both PIB MMs were confirmed by ^{1}H and ^{13}C NMR. Figures 1B and 1C show the ^{1}H NMR spectra of the oxanorbornene and norbornene MMs, respectively. Quantitative substitution of primary bromide for oxanorbornene is demonstrated in Figure 1B by the appearance of resonances with the theoretically predicted intensities at 6.50 (s), 5.25 (s), and 2.82 (s) ppm corresponding to vinyl, C_1/C_4 bridgehead, and C_2/C_3 bridgehead protons, respectively, of the oxanorbornene moiety. Similarly, evidence of quantitative conversion to PIB norbornene was demonstrated in Figure 1C by resonances of appropriate intensity appearing at 6.29 (s), 3.28 (s), and 2.68 (s) ppm due to vinyl, C_1/C_4 bridgehead, and C_2/C_3 bridgehead protons, respectively, of the norbornene moiety.

^{13}C NMR spectroscopy further verified the structures for both MMs (Figure S3A,B). For example, in Figure S3A, peaks at 176.3, 136.7, 81.1, and 47.6 ppm correspond to the carbonyl, alkene, C_1/C_4 bridgehead methine, and C_2/C_3 bridgehead methine carbons, respectively. With respect to the norbornene MM (Figure S3B), the major differences observed were the appearance of the methylene peak of the carbon bridge at 48.0 ppm and the upfield shift of the C_1/C_4 methine carbons to 43.0 ppm.

Number-average molecular weights (M_n) and $Đ$ of the PIB Br precursor and both PIB (oxa)norbornene MMs were measured by SEC, as shown in Figure S4, and the results are listed in Table S1 along with the M_ns calculated by NMR. Results from the two measurement methods were in close agreement. The SEC elution curves (refractive index traces) for the (oxa)norbornene derivatives were nearly identical to the PIB Br precursor, indicating that no chain coupling or degradation occurred during postpolymerization modification.

MALDI-TOF MS provided a second method to determine M_n, $Đ$, and end-functionality. The MALDI-TOF mass spectra of monofunctional PIB oxanorbornene and PIB norbornene MMs are shown in Figures 2A and 2B, respectively. Each

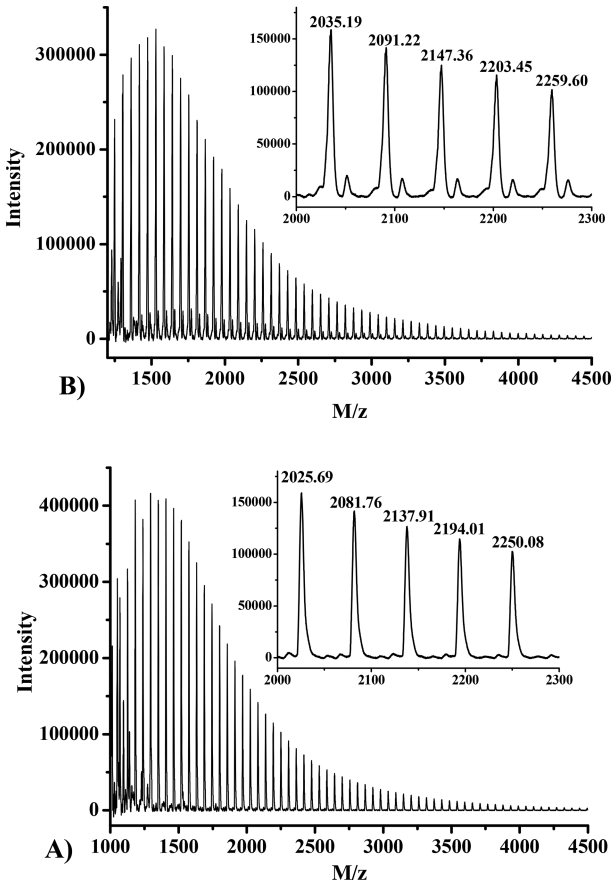

Figure 2. MALDI-TOF mass spectra of monofunctional (A) PIB oxanorbornene and (B) PIB norbornene MMs prepared by the dried droplet method using DCTB as the matrix, AgTFA as the cationizing agent, and THF as the solvent.

sample displays a single, major distribution of polymeric species, associated with Ag cations from the AgTFA cationizing agent, differing only by the number of isobutylene repeat units. The PIB norbornene MM sample also displayed a weak, secondary distribution. The data from each mass spectrum were analyzed by linear regression of a plot of mass-to-charge ratio (M/z, with z assumed to be 1), measured at the maximum of each peak of the major distribution, versus degree of polymerization (M/z vs DP plot).[59]

DOI: 10.1021/acs.macromol.7b01655
Macromolecules 2017, 50, 7458−7467

Table 1. Summary of ROMP of PIB MMs

			^{1}H NMR			SEC					
expt	MM	[MM]/[G3]	k_{app}[a] (min^{-1})	$t_{1/2}$[b] (min)	final p_{NMR}[c]	k_{app}[d] (min^{-1})	$t_{1/2}$[b] (min)	final p_{SEC}^{app}[e]	BB M_n[f] (Da × 10^{-5})	BB $M_{n,theo}$[g] (Da × 10^{-5})	$Đ$
1	MM1	100	0.14	4.95	0.97	0.08	8.66	0.89	4.0	401	1.03
2	MM2	100	0.40	1.73	0.97	0.26	2.66	0.87	3.9	392	1.01
3	MM2	50						0.90	2.0	202	1.02
4	MM2	75						0.89	3.1	300	1.01
5	MM2	100						0.89	4.1	400	1.01
6	MM2	125						0.88	5.4	495	1.02
7	MM2	150						0.89	7.1	601	1.04

[a]Slope of semilogarithmic plot from ^{1}H NMR data (Figure 3B). [b]Calculated using equation $t_{1/2} = \ln 2/k_{app}$. [c]Conversion of final aliquot measured in terms of norbornene olefin consumption from ^{1}H NMR data (Figure 3A). [d]Slope of semilogarithmic plot from SEC data (Figure 6B). [e]Conversion of final aliquot from SEC data, measured as $(A_{BB} + A_{MM})/A_{MM}$, where A_{BB} and A_{MM} are the integrated peak areas of the bottlebrush and macromonomers peaks in the RI trace; residual macromonomer fraction, f_{res}, was calculated using the equation $f_{res} = (1 - \text{final conv})$. [f]Measured by SEC using absolute MW determined by light scattering. [g]Calculated from SEC data using the formula $M_{n,theo} = M_{n,MM} \times \text{final } p_{SEC}^{app} \times ([MM]_0/[G3]_0)$.

MALDI-TOF MS data for the PIB (oxa)norbornene MMs are summarized in Table S2. For PIB norbornene MM, the measured slope value was within 0.1% of the theoretical molecular weight of the repeat unit (M_{ru}) (56.06 Da), and the measured intercept value was within 0.6% of the theoretical value of $EG + I + C$. The observed close agreement between measured and theoretical values provides strong evidence that the PIB norbornene MM possesses the targeted structure and end-group functionality. Analysis of the weak, secondary distribution revealed that its end-group mass was inconsistent with any likely structures, such as residual PIB-Br, and thus we were unable to provide a positive assignment. For PIB oxanorbornene MM, the measured slope value was within about 0.1% of the theoretical molecular weight of the repeat unit (M_{ru}) (56.06 Da), but the intercept differed from the theoretical value by about 1.8%, prompting further analysis. An overlay of the mass spectra of PIB oxanorbornene and PIB norbornene (Figure S5) showed that the individual homologues of the two distributions differ significantly in mass, whereas they should differ by only 2 Da (O vs CH_2). On the basis of the observed difference of about 66 Da, we have postulated that retro-Diels–Alder fragmentation of the oxanorbornene moiety occurred during the MALDI-TOP MS experiment. Thus, the observed distribution in the mass spectrum of PIB oxanorbornene was actually that of PIB maleimide. The theoretical value of $EG + I + C$ for the latter species is 450.12 Da, and the measured intercept of the M/z vs DP plot is within 0.6% of this value.

M_n and $Đ$ were also obtained from the mass spectroscopy data. In all cases, these values were lower than the corresponding values obtained from SEC analysis (Table S1). This is a common observation and reflects the fact that polymer chains with higher MW are more difficult to desorb/ionize and thus are under-represented at the detector.[47,48]

ROMP of PIB (Oxa)norbornene Macromonomers and ^{1}H NMR Kinetics Analysis. Controlled/"living" ROMP of PIB oxanorbornene (PIB MM1) and PIB norbornene (PIB MM2) was carried out using G3 catalyst owing to its improved functional group tolerance and high relative rates of initiation and propagation.[11−13] Aliquots were removed from the polymerization reactions at various times and terminated with ethyl vinyl ether. Each aliquot was subjected to both ^{1}H NMR and SEC analysis. As shown in the ^{1}H NMR spectra in Figure S6A,B, high norbornene conversion was achieved for both PIB MMs as evidenced by the disappearance of the alkene proton peaks at 6.50 and 6.29 ppm for PIB MM1 and PIB MM2, respectively, as well as the increase in intensity of peaks at 5.00−5.90 ppm, which correspond to the *cis* and *trans* double bonds of the polynorbornene backbone of the bottlebrush polymer. ^{1}H NMR data were used to provide a quantitative measure of macromonomer conversion, p_{NMR}, by monitoring the integration of (oxa)norbornene olefinic protons relative to that of the aromatic protons from the phenoxy moiety of the MMs, which remains constant. Conversions obtained from ^{1}H NMR were used to calculate propagation rate constants and reaction half-lives (Table 1). The conversion vs time plots (Figure 3A) show that the polymerization rate of PIB MM2 is faster than that of PIB MM1 as the conversion of PIB MM2 reached 97% in 8.7 min, while it took 24.6 min for PIB MM1 to achieve a similar conversion.

The semilogarithmic kinetic plots (Figure 3B) showed a linear relationship between $\ln[1/(1 - p_{NMR})]$ and reaction time, indicating G3 catalyst-mediated ROMP proceeds in a pseudo-first-order, controlled/"living" fashion. The slope for PIB MM2, i.e., the apparent first-order rate constant, was 2.9 times greater than that for PIB MM1. This result confirms the slower rates of ROMP of oxanorbornene as compared to analogous norbornene derivatives. The ether bridge within the oxanorbornene moiety plays an essential role in slowing the rate of propagation.[56] The ether oxygen is a strong electron-donating group, which coordinates with the electrophilic Ru and thus competes with the insertion of oxanorbornene olefin into Ru=C. However, despite the reduced ROMP rate of PIB MM1 near-quantitative (97%) oxanorbornene conversion was reached within about 25 min.

SEC Kinetics Analysis. An alternative kinetic study was conducted using an SEC technique.[11,12] Figures 4A and 4B illustrate SEC refractive index (RI) traces of aliquots removed from the ROMP of PIB MM1 and MM2 at various times, respectively. The data clearly demonstrate that as the reaction proceeds, the MM peak area decreases steadily, while the brush peak area steadily increases and shifts to lower elution volume. An apparent SEC conversion, p_{SEC}^{app}, may be determined at each aliquot by dividing the integrated area of the bottlebrush polymer peak, A_{BB}, by the sum of A_{BB} plus the area of the MM peak, A_{MM}:

DOI: 10.1021/acs.macromol.7b01655
Macromolecules 2017, 50, 7458−7467

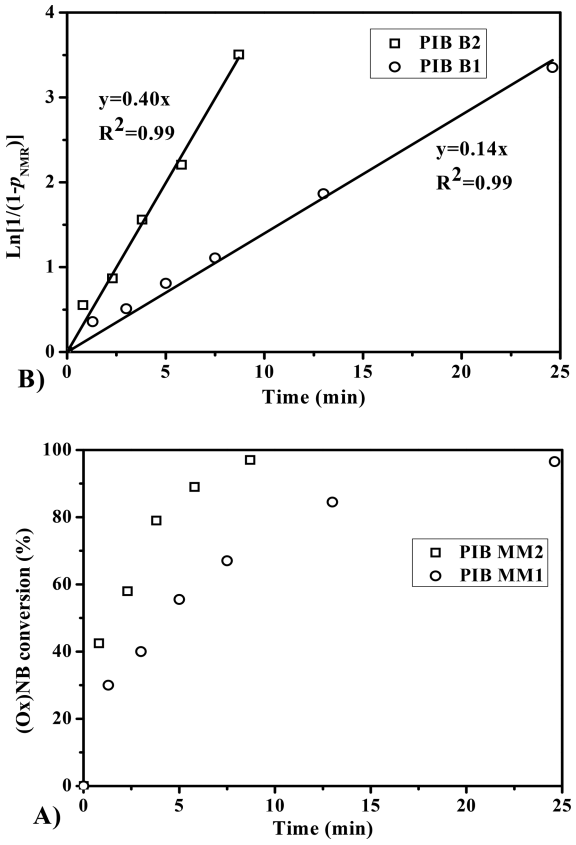

Figure 3. Kinetics of ROMP of PIB MM1 and PIB MM2 with G3 catalyst from ^{1}H NMR data ($[MM]_0$:$[G3]_0$ = 100:1, mol:mol), in CH_2Cl_2 at room temperature: (A) conversion (p_{NMR}) vs time plot; (B) semilogarithmic kinetic plots.

$$p_{SEC}^{app} = \frac{A_{BB}}{A_{BB} + A_{MM}} \quad (1)$$

We noted, however, that the SEC traces at long times appeared to approach a persistent, residual fraction of unreacted macromonomer. Other investigators have observed similar unreacted macromonomer fractions and attributed them to nonfunctional oligomers that are missing a polymerizable end group.[6,12] An alternative explanation is that the macromonomers are fully functionalized, and the unreacted macromonomer fraction represents a thermodynamically controlled equilibrium concentration. In either case, p_{SEC}^{app} may be converted to a true SEC conversion, p_{SEC}, through determination of the fraction of residual nonfunctional macromonomers, f_{res}:

$$p_{SEC} = \frac{p_{SEC}^{app}}{1 - f_{res}} \quad (2)$$

It should be noted that conversion measured by ^{1}H NMR, p_{NMR}, is inherently a true conversion since disappearance of the polymerizable norbornene olefin is being directly monitored.

We next conducted a series of polymerizations in which the G3 initiator concentration was systematically varied to produce different $[MM2]_0/[G3]_0$ ratios; PIB MM2 macromonomers were chosen due to their higher rate of propagation. This series was carried out in part to determine whether the apparent residual fraction of macromonomer discussed above was due to nonfunctional oligomers or equilibrium conditions or perhaps

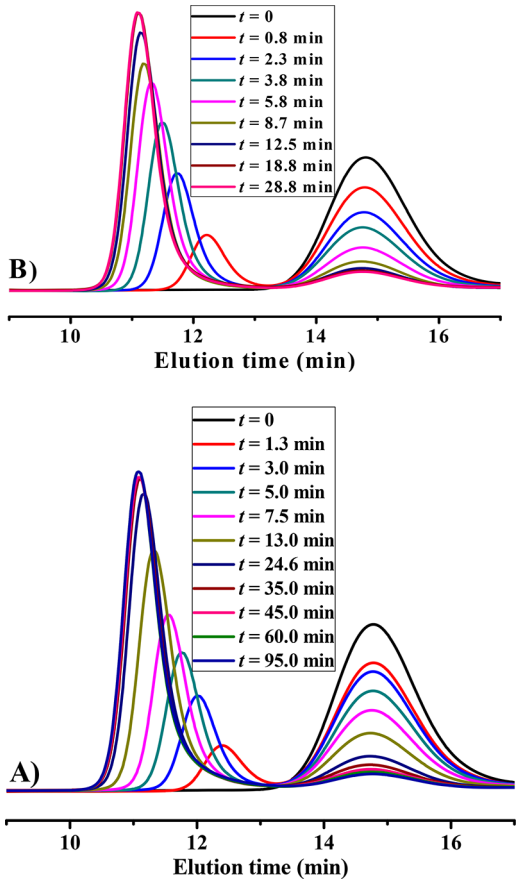

Figure 4. SEC traces of aliquots taken during ROMP of (A) PIB MM1, expt 1, Table 1, and (B) PIB MM2 using G3 catalyst, expt 2, Table 1; the peak at about 14.8 min corresponds to unreacted macromonomer.

to some other cause such as limited catalyst lifetime[12] or inadequate reaction time. If limited catalyst lifetime were the cause, then the residual fraction would most likely vary with $[G3]_0$. A relatively long reaction time of 1 h was used to ensure that macromonomer conversion was not being limited by ROMP kinetics. The results of this series of experiments are listed in Table 1, and the SEC RI traces of the final reaction products are shown in Figure 5A. M_ns of the resulting bottlebrush polymers were observed to be precisely controlled by the molar ratio of $[MM]_0/[G3]_0$, and the SEC curves were narrow and monomodal, demonstrating the high initiation efficiency and absence of chain transfer characteristic of ROMP mediated by the G3 catalyst. A plot of M_n vs molar feed ratio (Figure 5B) was observed to be linear and to pass through the origin, and the slope was approximately equal to the M_n of the starting PIB MM2, further confirming the controlled/living nature of the polymerization.

As determined by peak integration of the SEC traces in Figure 5A, the p_{SEC}^{app} was about 89% in all cases (data listed in Table 1), indicating that f_{res} assumed a constant value of about 11 mol % irrespective of $[G3]_0$. The constancy of this residual fraction, in spite of the widely varying $[PIB\ MM2]_0/[G3]_0$ ratios used, is consistent with a nonfunctional PIB fraction or a thermodynamically controlled equilibrium macromonomer concentration. MALDI-TOF-MS and especially NMR characterization of the PIB oligomers did not reveal any nonfunctional end groups, of which for PIB there are only a small

DOI: 10.1021/acs.macromol.7b01655
Macromolecules 2017, 50, 7458−7467

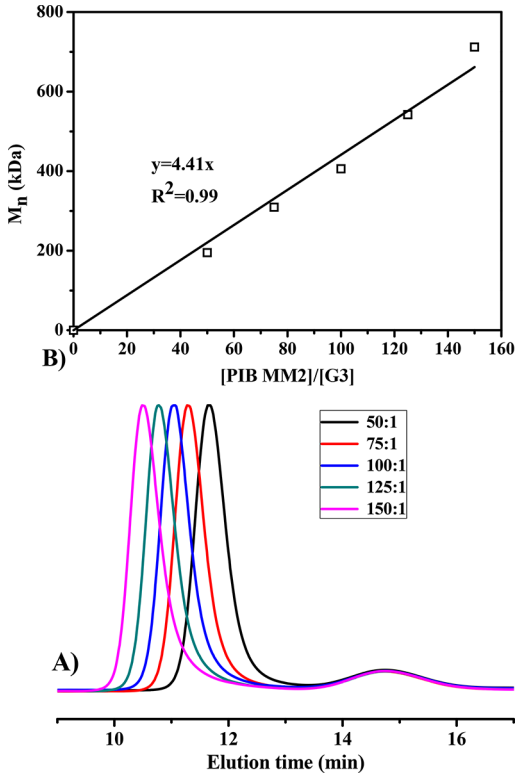

Figure 5. (A) SEC traces of ROMP of PIB MM2 at various $[MM2]_0/[G3]_0$ ratios after 1 h of reaction (expts 3−7, Table 1). (B) M_n vs $[PIB\ MM2]_0/[G3]_0$ feed ratio.

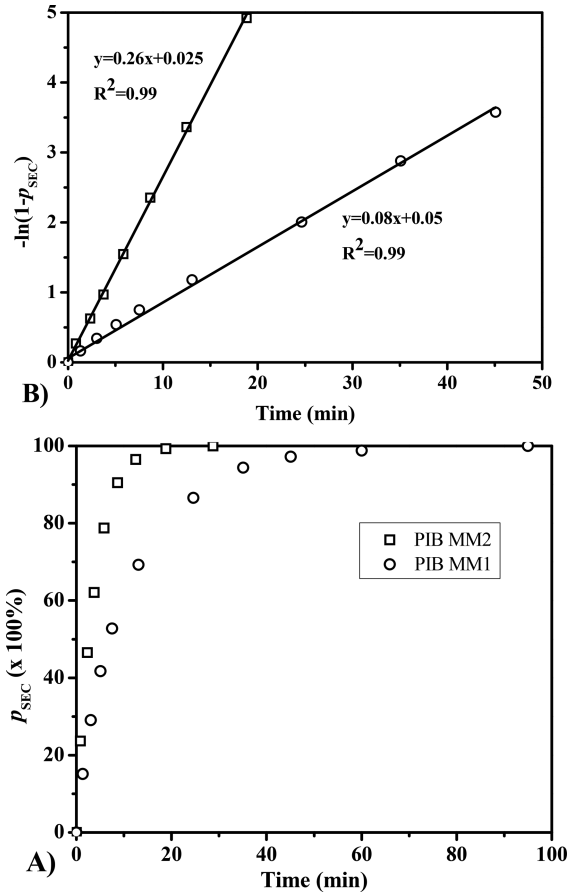

Figure 6. Kinetics of ROMP of PIB MM1 and PIB MM2 using G3 catalyst (MM:G3 = 100:1 (mol:mol), in CH_2Cl_2, at room temperature): (A) conversion vs time plots and (B) semilogarithmic kinetic plots.

number of characteristic types, e.g., *tert*-chloride, *exo*-olefin, *endo*-olefin, coupled. It is conceivable, however, that a fraction of the PIB chains initiated from the monofunctional initiator, TMPCl, which is slightly slow initiating, could have undergone rearrangement or isomerization of the carbocationic chain ends to form sterically hindered and less reactive chain ends,[60,61] resulting in incomplete conversion of PIB-Br by end quenching. At low concentration (~11 mol %) these end groups might not be revealed in ^{1}H NMR, even at 600 MHz resolution, and the resulting nonfunctional PIB chains would remain unreactive toward (oxa)norbornene precursors and thence the G3 catalyst during ROMP.

Conversion vs time (Figure 6A) and semilogarithmic kinetic plots (Figure 6B) were constructed from SEC data for aliquots removed from ROMP of PIB MM1 and PIB MM2 (expts 1 and 2, respectively, Table 1). For these plots, true SEC conversion, p_{SEC}, was measured using eqs 1 and 2 with f_{res} assumed to be 0.11 for both macromonomers. Apparent propagation rate constants and half-lives were calculated from the slopes of semilogarithmic kinetic plots and are listed in Table 1. The data demonstrate the same relative trends observed in the ^{1}H NMR kinetics analysis; however, the rate constants measured by SEC were lower than those by NMR. Measured by SEC, the apparent first-order rate constant for PIB MM2 was 3.25 times greater than that for PIB MM1.

CONCLUSIONS

Novel PIB (oxa)norbornene MMs were prepared by reacting *exo*-(oxa)norbornene imide with PIB-Br. G3 catalyst-mediated "controlled"/living ROMP of PIB (oxa)norbornene MMs via a grafting "through" methodology was conducted successfully at room temperature, producing PIB bottlebrush polymers with precisely controlled MWs and low $Đ$ (≤1.04). It was demonstrated that PIB brushes with high MW (700 kDa) could be achieved by varying the feed ratio of the $[(oxa)\text{-}norbornene]_0/[G3]_0$; even higher MW could very likely be achieved by further increasing the latter ratio, since no termination or G3 catalyst degradation was observed even at very high MM conversions. It was demonstrated that the ROMP propagation rate of PIB norbornene is at least 2.9 times greater than that of PIB oxanorborne MM with similar MW, owning to the complex effect between the electron-rich oxygen atom and G3, which interfered with but did not inhibit the interaction of Ru=C with the polymerizable oxanorbornene moiety.

ROMP of PIB (oxa)norbornene MMs represents an effective, fast, and facile method for the preparation of PIB brushes. Owing to the exceptional properties of PIB itself, such as good flexibility and damping, good thermal and oxidative stability, chemical and solvent resistance, and biocompatibility, PIB brushes have the potential to be applied in the fields of rheology modifiers, supersoft elastomers, vibration or noise damping materials, and polymer therapeutics.

EXPERIMENTAL SECTION

Materials. Hexane (anhydrous, 95%), methanol (anhydrous, 99.8%), methylene chloride (anhydrous, 99.8%), titanium tetrachloride ($TiCl_4$) (99.9%), 2,6-lutidine (99.5%), anisole (anhydrous, 99.7%), (3-bromopropoxy)benzene (anhydrous, 98%), tetrahydrofur-

DOI: 10.1021/acs.macromol.7b01655
Macromolecules 2017, 50, 7458−7467

an (THF) (anhydrous, 99.9%), ethyl vinyl ether (99%), maleimide (99%), pentane, dichloromethane-d_2 (CD_2Cl_2), diethyl ether, furan (99%), second-generation Grubbs catalyst, pyridine (99%), potassium carbonate (K_2CO_3), ethyl acetate (99%), maleic anhydride (99%), dicyclopentadiene (99%), urea (99%), toluene (99%), 1,2-dichlorobenzene, and silver trifluoroacetic acid (AgTFA) were purchased from Sigma-Aldrich and used as received. *trans*-2-[3-(4-*t*-Butylphenyl)-2-methyl-2-propenylidene]malononitrile (DTCB) was purchased from Tokyo Chemical Industry Co. and used as received. Magnesium sulfate ($MgSO_4$) (anhydrous), sulfuric acid (98%), and chloroform-d ($CDCl_3$) were purchased and used as received from Fisher Scientific. Acetonitrile-d_3 (99.8%) was purchased from Cambridge Isotopes and used as received. Isobutylene (IB, BOC Gases) and methyl chloride (Gas and Supply) were dried by passing the gaseous reagent through a column of $CaSO_4$/molecular sieves/$CaCl_2$ and condensing within a N_2-atmosphere glovebox immediately prior to use. The monofunctional initiator, 2-chloro-2,4,4-trimethylpentane (TMPCl), was synthesized as previously described[62] by bubbling HCl gas through neat 2,4,4-trimethyl-1-pentene (Sigma-Aldrich Co.) at 0 °C and was stored at 0 °C prior to use.

Instrumentation. Nuclear magnetic resonance (^{1}H NMR and ^{13}C NMR) experiments were performed on a Varian 300 MHz or a Bruker Ascend 600.13 MHz (TopSpin 3.5) spectrometer. All ^{1}H chemical shifts were referenced to TMS (0 ppm), and all ^{13}C shifts were referenced to $CDCl_3$ (77.16 ppm). Samples were prepared by dissolving the polymer in either chloroform-*d* or acetonitrile-d_3 (5−7%, w/v) and charging this solution to a 5 mm NMR tube. For quantitative proton integration, 16 transients were acquired using a pulse delay of 27.3 s. In the end-group analysis, the signal due to the ultimate methylene protons adjacent to the phenoxy moiety (1.79 ppm, 2H, singlet) was chosen as an internal reference for functionality analysis.

Real-time Fourier transform infrared (RT-FTIR) monitoring of isobutylene polymerizations was performed using a ReactIR 45m (Mettler-Toledo) integrated with a N_2-atmosphere glovebox (MBraun Labmaster 130) equipped with a cryostated heptane bath. Isobutylene conversion during polymerization was determined by monitoring the area above a two-point baseline of the absorbance at 887 cm^{-1}, associated with the $=CH_2$ wag of isobutylene.

Number-average molecular weights (M_n) and polydispersities (PDI = M_w/M_n) were determined using a gel-permeation chromatography (GPC) system consisting of a Waters Alliance 2695 separations module, an online multiangle laser light scattering (MALLS) detector fitted with a gallium arsenide laser (power: 20 mW) operating at 658 nm (miniDAWN TREOS, Wyatt Technology Inc.), an interferometric refractometer (Optilab rEX, Wyatt Technology Inc.) operating at 35 °C and 685 nm, and two PLgel columns (Polymer Laboratories Inc.) connected in series. For characterization of macromonomers, two mixed E columns (pore size range 50−10^3 Å, 3 μm bead size) were used; for the bottlebrush polymers, two mixed D columns (pore size range 50−10^4 Å, 5 μm bead size) were used. Freshly distilled THF served as the mobile phase and was delivered at a flow rate of 1.0 mL/min. Sample concentrations were ca. 15−20 mg of polymer/mL of THF, and the injection volume was 100 μL. The detector signals were simultaneously recorded using ASTRA software (Wyatt Technology Inc.), and absolute molecular weights were determined by MALLS. For PIB macromonomers dn/dc was calculated from the refractive index detector response and assuming 100% mass recovery from the columns; for PIB bottlebrush polymers, the dn/dc was set to the known value for PIB of 0.1080 mL/g.

Matrix-assisted laser desorption/ionization time-of-flight mass spectrometry (MALDI-TOF MS) was performed using a Bruker Microflex LRF MALDI-TOF mass spectrometer equipped with a nitrogen laser (337 nm) possessing a 60 Hz repetition rate and 50 μJ energy output. The PIB samples were prepared using the dried droplet method: separately prepared THF solutions of DCTB matrix (20 mg/mL), PIB sample (10 mg/mL), and AgTFA cationizing agent (10 mg/mL) were mixed in a volumetric ratio of matrix/sample/cationizing agent = 4:1:0.2, and a 0.5 μL aliquot was applied to a MALDI sample target for analysis. The spectrum was obtained in the positive ion mode utilizing the Reflector mode microchannel plate detector and was generated as the sum of 900−1000 shots.

*exo-7-Oxanorbornene-2,3-dicarboximide (**1**).* Precursor **1** was synthesized using a variation of a published procedure.[63,64] A solution of maleimide (4.75 g, 48.9 mmol) and freshly distilled furan (25.0 mL, 343 mmol) in EtOAc (100 mL) was prepared in a 250 mL three-necked round-bottomed flask equipped with magnetic stir bar and reflux condenser. The reaction was purged with N_2 for 30 min and then heated at 80 °C overnight (18 h). The reaction was then cooled to room temperature, and pentane (50 mL) was added, followed by cooling to −10 °C for 6 h affording **1** (6.69 g, 83%) as colorless crystals; mp 168−170 °C dec. ^{1}H NMR (300 MHz, CD_3CN): δ 8.88 (s, 1H), 6.49 (s, 2H), 5.14 (s, 2H), 2.84 (s, 2H). ^{13}C NMR (75 MHz, CD_3CN): δ 178.34, 137.78, 82.24, 50.02.

*exo-5-Norbornene-2,3-dicarboxylic Anhydride (**2a**).* A 500 mL three-necked round-bottomed flask equipped with a magnetic stir bar, condenser, and addition funnel was charged with maleic anhydride (98.06 g, 1.00 mol) and 1,2-dichlorobenzene (100 mL) and heated to 200 °C. Subsequently, a solution of dicyclopentadiene (69.41 g, 0.525 mol) in 1,2-dichlorobenzene (40 mL) was added dropwise over 1 h while maintaining the reaction temperature at 200 °C. The reaction was then heated at 230 °C for 2.5 h, followed by cooling to room temperature (12 h). The resulting crystals were isolated by vacuum filtration and recrystallized three additional times from toluene to give **2a** (46.4 g, 28%) as needlelike crystals. ^{1}H NMR (300 MHz, $CDCl_3$): δ 6.29 (s, 2H), 3.41 (s, 2H), 2.97 (s, 2H), 1.63 (d, J = 9.8 Hz, 1H), 1.40 (d, J = 10.1 Hz, 1H).

*exo-5-Norbornene-2,3-dicarboximide (**2**).* Intermediate **2a** (41.20 g, 251 mmol) and urea (16.58 g, 276 mmol) were weighed into a 250 mL round bottomed flask equipped with magnetic stir bar and reflux condenser. The reactor was evacuated of air and backfilled with argon and then heated at 150 °C for 2 h. Melting of the reactants was accompanied by vigorous evolution of gas, which was vented through an oil bubbler. The crude product was purified by dissolving in water (700 mL) at 90 °C, followed by recrystallization at room temperature giving **2** (31.60 g, 77%) as off-white crystals that were dried overnight *in vacuo*; mp 163−164 °C. ^{1}H NMR (300 MHz, $CDCl_3$): δ 8.57 (s, 1H), 6.26 (s, 2H), 3.27 (s, 2H), 2.71 (s, 2H), 1.55 (d, J = 10.0 Hz, 1H), 1.43 (d, J = 9.6 Hz, 1H). ^{13}C NMR (75 MHz, $CDCl_3$): δ 178.76, 137.94, 49.36, 45.31, 43.10.

*Third-Generation Grubbs Catalyst (G3, **3**).* Second-generation Grubbs catalyst (500 mg, 0.12 mmol) was weighed into a scintillation vial containing a small magnetic stir bar followed by the addition of pyridine (0.474 mL, 5.88 mmol) in the presence of air. After 5 min, pentane (20 mL) was added to the vial resulting in precipitation of a bright green solid. The vial was placed in the refrigerator (5 °C) overnight. The green G3 catalyst (**3**) was isolated by vacuum filtration, washed with pentane (20 mL), dried *in vacuo*, and subsequently stored under argon in the dark at 5 °C. Yield: 400 mg, 93%.

Monofunctional Primary Bromide-Terminated PIB Precursor (PIB-Br). Monofunctional PIB Br precursor was synthesized by living isobutylene polymerization/alkoxybenzene quenching. Polymerization and quenching reactions were performed within a N_2-atmosphere glovebox equipped with a cryostated heptane bath. Synthesis of 4K PIB Br was carried out as follows: To a 1 L four-neck round-bottom flask, equipped with an overhead stirrer, thermocouple, and ReactIR probe, and immersed in the heptane bath, were added 131 mL of hexane, 196 mL of methyl chloride, 0.15 mL (1.3 mmol) of 2,6-lutidine, 3.40 mL (20.0 mmol, 2.97 g) of TMPCl, and 105 mL (1.31 mol) of IB. The mixture was equilibrated to −70 °C with stirring, and polymerization was initiated by the addition of 0.82 mL (7.5 mmol) of $TiCl_4$. Essentially full monomer conversion was reached in 42 min according to RT-FTIR data, at which time 9.5 mL (60.0 mmol) of 3-bromopropoxybenzene was charged to the reaction (3 equiv per chain end). Additional $TiCl_4$ (3.67 mL, 33.4 mmol) was added to catalyze the quenching reaction, resulting in a total $TiCl_4$ concentration of 2 equiv per chain end. The quenching reaction was allowed to proceed for 5 h. At the end of this time, the catalyst was destroyed by careful addition of excess prechilled methanol (~30 mL). The resulting polymer solution was washed with methanol and then precipitated

DOI: 10.1021/acs.macromol.7b01655
Macromolecules 2017, 50, 7458−7467

into 1.5 L of methanol and acetone solution (methanol/acetone, v/v, 95/5). The precipitate was collected by redissolution in fresh hexane; the solution was washed with DI water, dried over $MgSO_4$, and then vacuum stripped. Residual solvent was removed under vacuum at 50 °C to yield pure primary bromide-terminated PIB (M_n = 4200 g/mol, $Đ$ = 1.23).

Monofunctional PIB Oxanorbornene (PIB MM1) and PIB Norbornene (PIB MM2) Macromonomers. Monofunctional primary bromide-terminated PIB precursor (PIB Br, 15.1 g, M_n = 4200 g/mol, PDI = 1.23) was dissolved in 200 mL of freshly distilled THF, and the resulting solution was transferred to a 500 mL one-neck round-bottom flask. To the stirred solution were added 40 mL of anhydrous *N*-methyl-2-pyrrolidone (NMP), 1.77 g (10.8 mmol) of *exo*-5-norbornene-2,3-dicarboximide (**2**), 2.47 g (17.9 mmol) of potassium carbonate, and 1.89 g (7.16 mmol) of 18-crown-6. The mixture was heated at 50 °C under a dry N_2 atmosphere for 10 h. Upon completion of the reaction, the THF was vacuum stripped, and the polymer was dissolved in hexane. The resulting solution was filtered through a filter paper and slowly added into excess methanol to precipitate the polymer. The precipitate was redissolved in fresh hexane, and the resulting solution was washed with DI water, dried over $MgSO_4$, and then vacuum stripped at room temperature to obtain pure PIB MM2 (M_n = 4500 g/mol, $Đ$ = 1.21). PIB MM1 prepolymer (M_n = 4500 g/mol, $Đ$ = 1.22) was prepared using a similar procedure.

PIB Bottlebrushes via ROMP of *exo*-(Oxa)norbornene-Functional PIB. ROMP was carried out in a mixed 9:1 (v:v) CH_2Cl_2:hexane cosolvent system at room temperature. A representative procedure was as follows: PIB MM2 (500 mg, 1.1×10^{-4} mol, 100 equiv) and 4.0 mL of a 9:1 (v:v) mixture of CH_2Cl_2 and hexane were charged to a vial equipped with magnetic stir bar and septum cap. Upon dissolution of the polymer, the vial was degassed via four freeze−pump−thaw cycles and backfilled with argon. Meanwhile, a stock solution of G3 was prepared in a separate vial equipped with septum cap. G3 (9.05 mg) was charged to the vial; the vail was evacuated/refilled with argon four times, and 1.0 mL of previously degassed 9:1 (v:v) CH_2Cl_2:hexane (4 × freeze−pump−thaw cycles) was added to the vial using an argon-purged gastight syringe. The polymerization was initiated by the addition of 89 μL of G3 stock solution (1.1×10^{-6} mol, 1 equiv) to the vial of PIB MM2 using an argon-purged gastight syringe. Aliquots (50 μL) were taken from the reaction at timed intervals and terminated by addition to separate vials containing 300 μL of CH_2Cl_2 and 2−3 drops of ethyl vinyl ether.

PIB Bottlebrushes via ROMP of *exo*-Norbornene-Functional PIB with Various MW. PIB MM2 was used to prepare a series of PIB bottlebrush polymers with various MW by maintaining a constant concentration of PIB MM2 and varying the concentration of G3 to achieve molar ratio of $[PIB\ MM2]_0/[G3]_0$ at 50:1, 75:1, 100:1, 125:1, and 150:1. A representative procedure was as follows: PIB MM2 (200 mg, 4.4×10^{-5} mol, 50 equiv) and 1.6 mL of a 9:1 (v:v) mixture of CH_2Cl_2 and hexane were charged to a vial equipped with magnetic stir bar and septum cap. Upon dissolution of the polymer, the vial was degassed via four freeze−pump−thaw cycles and backfilled with argon. The polymerization was initiated by the addition of 70 μL of the G3 stock solution described above (8.8×10^{-7} mol, 1 equiv) to the vial of PIB MM2 using an argon-purged gastight syringe. The reaction was allowed to proceed for 1 h to ensure complete macromonomer conversion and then terminated by addition to separate vials containing 300 μL of CH_2Cl_2 and 2−3 drops of ethyl vinyl ether.

■ ASSOCIATED CONTENT

Supporting Information

The Supporting Information is available free of charge on the ACS Publications website at DOI: 10.1021/acs.macromol.7b01655.

Additional data (NMR spectra, SEC data, MALDI-TOF MS data, kinetic data) (PDF)

■ AUTHOR INFORMATION

Corresponding Author

*E-mail: Robson.Storey@usm.edu (R.F.S.).

ORCID

Robson F. Storey: 0000-0002-7747-762X

Present Addresses

B.Y.: Corning Incorporated, 1 Science Center Dr., Painted Post, NY 14870.

B.A.A.: Department of Chemistry and Chemical Biology, Baker Laboratory, Cornell University, Ithaca, NY 14853-1301.

Notes

The authors declare no competing financial interest.

■ ACKNOWLEDGMENTS

This research was supported in part by the National Science Foundation Experimental Program to Stimulate Competitive Research (EPSCoR) under Cooperative Agreement No. IIA1430364. The authors also thank Dr. William Jarrett for assistance with NMR spectroscopy and Richard Cooke, Logan Dugas, and Jie Wu of the Storey Research Group for their assistance in acquisition and interpretation of MALDI-TOF MS data.

■ REFERENCES

(1) Lee, H.-i.; Pietrasik, J.; Sheiko, S. S.; Matyjaszewski, K. Stimuli-Responsive Molecular Brushes. *Prog. Polym. Sci.* **2010**, *35* (1−2), 24−44.

(2) Sheiko, S. S.; Sumerlin, B. S.; Matyjaszewski, K. Cylindrical Molecular Brushes: Synthesis, Characterization, and Properties. *Prog. Polym. Sci.* **2008**, *33* (7), 759−785.

(3) Yuan, J.; Lu, Y.; Schacher, F.; Lunkenbein, T.; Weiss, S.; Schmalz, H.; Müller, A. H. E. Template-Directed Synthesis of Hybrid Titania Nanowires within Core-Shell Bishydrophilic Cylindrical Polymer Brushes. *Chem. Mater.* **2009**, *21* (18), 4146−4154.

(4) Bolton, J.; Rzayev, J. Tandem RAFT-ATRP Synthesis of Polystyrene-Poly(methyl methacrylate) Bottlebrush Block Copolymers and Their Self-Assembly into Cylindrical Nanostructures. *ACS Macro Lett.* **2012**, *1* (1), 15−18.

(5) Pesek, S. L.; Li, X.; Hammouda, B.; Hong, K.; Verduzco, R. Small-Angle Neutron Scattering Analysis of Bottlebrush Polymers Prepared via Grafting-Through Polymerization. *Macromolecules* **2013**, *46* (17), 6998−7005.

(6) Dalsin, S. J.; Hillmyer, M. A.; Bates, F. S. Molecular Weight Dependence of Zero-Shear Viscosity in Atactic Polypropylene Bottlebrush Polymers. *ACS Macro Lett.* **2014**, *3* (5), 423−427.

(7) Verduzco, R.; Li, X.; Pesek, S. L.; Stein, G. E. Structure, Function, Self-Assembly, and Applications of Bottlebrush Copolymers. *Chem. Soc. Rev.* **2015**, *44* (8), 2405−2420.

(8) Nese, A.; Li, Y.; Averick, S.; Kwak, Y.; Konkolewicz, D.; Sheiko, S. S.; Matyjaszewski, K. Synthesis of Amphiphilic Poly(*N*-vinylpyrrolidone)-*b*-poly(vinyl acetate) Molecular Bottlebrushes. *ACS Macro Lett.* **2012**, *1* (1), 227−231.

(9) Li, Y.; Zou, J.; Das, B. P.; Tsianou, M.; Cheng, C. Well-Defined Amphiphilic Double_Brush Copolymers and Their Performance as Emulsion Surfactants. *Macromolecules* **2012**, *45* (11), 4623−4629.

(10) Iwawaki, H.; Urakawa, O.; Inoue, T.; Nakamura, Y. Rheo-Optical Study on Dynamics of Bottlebrush-Like Polymacromonomer Consisting of Polystyrene. II. Side Chain Length Dependence on Dynamical Stiffness of Main Chain. *Macromolecules* **2012**, *45* (11), 4801−4808.

(11) Ganewatta, M. S.; Ding, W.; Rahman, M. A.; Yuan, L.; Wang, Z.; Hamidi, N.; Robertson, M. L.; Tang, C. Biobased Plastics and Elastomers from Renewable Rosin via "Living" Ring-Opening Metathesis Polymerization. *Macromolecules* **2016**, *49* (19), 7155−7164.

DOI: 10.1021/acs.macromol.7b01655
Macromolecules 2017, 50, 7458−7467

(12) Radzinski, S. C.; Foster, J. C.; Chapleski, R. C., Jr.; Troya, D.; Matson, J. B. Bottlebrush Polymer Synthesis by Ring-Opening Metathesis Polymerization: The Significance of the Anchor Group. *J. Am. Chem. Soc.* **2016**, *138* (22), 6998−7004.
(13) Xia, Y.; Kornfield, J. A.; Grubbs, R. H. Efficient Synthesis of Narrowly Dispersed Brush Polymers via Living Ring-Opening Metathesis Polymerization of Macromonomers. *Macromolecules* **2009**, *42* (11), 3761−3766.
(14) Radzinski, S. C.; Foster, J. C.; Matson, J. B. Synthesis of Bottlebrush Polymers *via* Transfer-To and Grafting-Through Approaches Using a RAFT Chain Transfer Agent with a ROMP-Active Z-Group. *Polym. Chem.* **2015**, *6* (31), 5643−5652.
(15) Patton, D. L.; Advincula, R. C. A Versatile Synthetic Route to Macromonomers via RAFT Polymerization. *Macromolecules* **2006**, *39* (25), 8674−8683.
(16) Cheng, G.; Böker, A.; Zhang, M.; Krausch, G.; Müller, A. H. E. Amphiphilic Cylindrical Core-Shell Brushes via a "Grafting From" Process Using ATRP. *Macromolecules* **2001**, *34* (20), 6883−6888.
(17) Runge, M. B.; Dutta, S.; Bowden, N. B. Synthesis of Comb Block Copolymers by ROMP, ATRP, and ROP and Their Assembly in the Solid State. *Macromolecules* **2006**, *39* (2), 498−508.
(18) Helms, B.; Mynar, J. L.; Hawker, C. J.; Fréchet, J. M. J. Dendronized Linear Polymers via "Click Chemistry. *J. Am. Chem. Soc.* **2004**, *126* (46), 15020−15021.
(19) Gao, H.; Matyjaszewski, K. Synthesis of Molecular Brushes by "Grafting onto" Mehtod: Combination of ATRP and Click Reactions. *J. Am. Chem. Soc.* **2007**, *129* (20), 6633−6639.
(20) Schappacher, M.; Deffieux, A. Synthesis of Macrocyclic Copolymer Brushes and Their Self-Assembly into Supramolecular Tubes. *Science* **2008**, *319* (5869), 1512−1515.
(21) Dziezok, P.; Fischer, K.; Schmidt, M.; Sheiko, S. S.; Möller, M. Cylindrical Molecular Brushes. *Angew. Chem., Int. Ed. Engl.* **1997**, *36* (24), 2812−2815.
(22) Gerle, M.; Fischer, K.; Roos, S.; Müller, A. H. E.; Schmidt, M.; Sheiko, S. S.; Prokhorova, S.; Möller, M. Main Chain Conformation and Anomalous Elution Behavior of Cylindrical Brushes as Revealed by GPC/MALLS, Light Scattering, and SFM. *Macromolecules* **1999**, *32* (8), 2629−2637.
(23) Ito, K.; Tanaka, K.; Tanaka, H.; Imai, G.; Kawaguchi, S.; Itsuno, S. Poly(ethylene oxide) Macromonomers. 7. Micellar Polymerization in Water. *Macromolecules* **1991**, *24* (9), 2348−2354.
(24) Sveinbjörnsson, B. R.; Miyake, G. M.; El-Batta, A.; Grubbs, R. H. Stereocomplex Formation of Densely Grafted Brush Polymers. *ACS Macro Lett.* **2014**, *3* (1), 26−29.
(25) Radzinski, S. C.; Foster, J. C.; Matson, J. B. Preparation of Bottlebrush Polymers via a One-Pot Ring-Opening Polymerization (ROP) and Ring-Opening Metathesis Polymerization (ROMP) Grafting-Through Strategy. *Macromol. Rapid Commun.* **2016**, *37* (7), 616−621.
(26) Zhang, M.; Breiner, T.; Mori, H.; Müller, A. H. E. Amphiphilic Cylindrical Brushes with Poly(acrylic acid) Core and Poly(*n*-butyl acrylate) Shell and Narrow Length Distribution. *Polymer* **2003**, *44* (5), 1449−1458.
(27) Johnson, J. A.; Lu, Y. Y.; Burts, A. O.; Xia, Y.; Durrell, A. C.; Tirrell, D. A.; Grubbs, R. H. Drug-Loaded, Bivalent-Bottle-Brush Polymers by Graft-through ROMP. *Macromolecules* **2010**, *43* (24), 10326−10335.
(28) Li, Z.; Ma, J.; Cheng, C.; Zhang, K.; Wooley, K. L. Synthesis of Hetero-Grafted Amphiphilic Diblock Molecular Brushes and Their Self-Assembly in Aqueous Medium. *Macromolecules* **2010**, *43* (3), 1182−1184.
(29) Gregory, A.; Stenzel, M. H. Complex Polymer Architectures via RAFT Polymerization: From Fundamental Process to Extending the Scope Using Click Chemistry and Nature's Building Blocks. *Prog. Polym. Sci.* **2012**, *37* (1), 38−105.
(30) Sveinbjörnsson, B. R.; Weitekamp, R. A.; Miyake, G. M.; Xia, Y.; Atwater, H. A.; Grubbs, R. H. Rapid Self-Assembly of Brush Block Copolymers to Photonic Crystals. *Proc. Natl. Acad. Sci. U. S. A.* **2012**, *109* (36), 14332−14336.
(31) Teo, Y. C.; Xia, Y. Importance of Macromonomer Quality in the Ring-Opening Metathesis Polymerization of Macromonomers. *Macromolecules* **2015**, *48* (16), 5656−5662.
(32) Choi, T.-L.; Grubbs, R. H. Controlled Living Ring-Opening-Metathesis Polymerization by a Fast-Initiating Ruthenium Catalyst. *Angew. Chem., Int. Ed.* **2003**, *42* (15), 1743−1746.
(33) Bielawski, C. W.; Grubbs, R. H. Living Ring-Opening Metathesis Polymerization. *Prog. Polym. Sci.* **2007**, *32* (1), 1−29.
(34) Leitgeb, A.; Wappel, J.; Slugovc, C. The ROMP Toolbox Upgraded. *Polymer* **2010**, *51* (14), 2927−2946.
(35) Liu, J.; Burts, A. O.; Li, Y.; Zhukhovitskiy, A. V.; Ottaviani, M. F.; Turro, N. J.; Johnson, J. A. Brush-First" Method for the Parallel Synthesis of Photocleavable, Nitroxide-Labeled Poly(ethylene glycol) Star Polymers. *J. Am. Chem. Soc.* **2012**, *134* (39), 16337−16344.
(36) Kim, J. G.; Coates, G. W. Synthesis and Polymerization of Norbornenyl-Terminated Multiblock Poly(cyclohexene carbonate)s: A Consecutive Ring-Opening Polymerization Route to Multisegmented Graft Polycarbonates. *Macromolecules* **2012**, *45* (19), 7878−7883.
(37) Miyake, G. M.; Weitekamp, R. A.; Piunova, V. A.; Grubbs, R. H. Synthesis of Isocyanate-Based Brush Block Copolymers and Their Rapid Self-Assembly to Infrared-Reflecting Photonic Crystals. *J. Am. Chem. Soc.* **2012**, *134* (34), 14249−14254.
(38) Li, Y.; Themistou, E.; Zou, J.; Das, B. P.; Tsianou, M.; Cheng, C. Facile Synthesis and Visualization of Janus Double-Brush Copolymers. *ACS Macro Lett.* **2012**, *1* (1), 52−56.
(39) Cheng, C.; Khoshdel, E.; Wooley, K. L. One-Pot Tandem Synthesis of a Core-Shell Brush Copolymer from Small Molecule Reactants by Ring-Opening Metathesis and Reversible Addition-Fragmentation Chain Transfer (Co)polymerizations. *Macromolecules* **2007**, *40* (7), 2289−2292.
(40) Hawker, C. J.; Bosman, A. W.; Harth, E. New Polymer Synthesis by Nitroxide Mediated Living Radical Polymerizations. *Chem. Rev.* **2001**, *101* (12), 3661−3688.
(41) Matyjaszewski, K.; Xia, J. Atom Transfer Radical Polymerization. *Chem. Rev.* **2001**, *101* (9), 2921−2990.
(42) Sukegawa, T.; Masuko, I.; Oyaizu, K.; Nishide, H. Expanding the Dimensionality of Polymers Populated with Organic Robust Radicals toward Flow Cell Application: Synthesis of TEMPO-Crowded Bottlebrush Polymers Using Anionic Polymerization and ROMP. *Macromolecules* **2014**, *47* (24), 8611−8617.
(43) Al-Hashimi, M.; Bakar, M. D. A.; Elsaid, K.; Bergbreiter, D. E.; Bazzi, H. S. Ring-Opening Metathesis Polymerization Using Polyisobutylene Supported Grubbs Second-Generation Catalyst. *RSC Adv.* **2014**, *4* (82), 43766−43771.
(44) Malins, E. L.; Waterson, C.; Becer, C. R. Controlled Synthesis of Amphiphilic Block Copolymers Based on Poly(Isobutylene) Macromonomers. *J. Polym. Sci., Part A: Polym. Chem.* **2016**, *54* (5), 634−643.
(45) Erdodi, G.; Kennedy, J. P. Amphiphilic Conetworks: Definition, Synthesis, Applications. *Prog. Polym. Sci.* **2006**, *31* (1), 1−18.
(46) Tsou, A. H.; López-Barrón, C. R.; Jiang, P.; Crowther, D. J.; Zeng, Y. Bimodal Poly(ethylene-cb-propylene) Comb Block Copolymers from Serial Reactors: Synthesis and Applications as Processability Additives and Blend Compatibilizers. *Polymer* **2016**, *104* (8), 72−82.
(47) Roche, C. P.; Brei, M. R.; Yang, B.; Storey, R. F. Direct Chain End Functionalization of Living Polyisobutylene Using Phenoxyalkyl (Meth)acrylates. *ACS Macro Lett.* **2014**, *3* (12), 1230−1234.
(48) Yang, B.; Parada, C. M.; Storey, R. F. Synthesis, Characterization, and Photopolymerization of Polyisobutylene Phenol (Meth)-acrylate Macromers. *Macromolecules* **2016**, *49* (17), 6173−6185.
(49) Tripathy, R.; Ojha, U.; Faust, R. Synthesis and Characterization of Polyisobutylene Macromonomers with Methacrylate, Acrylate, Glycidyl Ether, or Vinyl Ether End-Functionality. *Macromolecules* **2009**, *42* (12), 3958−3964.
(50) Ojha, U.; Rajkhowa, R.; Agnihotra, S. R.; Faust, R. A New General Methodology for the Synthesis of End-Functional Polyisobutylenes by Nucleophilic Substitution Reactions. *Macromolecules* **2008**, *41* (11), 3832−3841.

DOI: 10.1021/acs.macromol.7b01655
Macromolecules 2017, 50, 7458−7467

(51) Yang, B.; Storey, R. F. End-Quenching of *tert*-Chloride-Terminated Polyisobutylene with Alkoxybenzenes: Comparison of $AlCl_3$ and $TiCl_4$ Catalyst. *Polym. Chem.* **2015**, *6* (20), 3764−3774.
(52) Morgan, D. L.; Martinez-Castro, N.; Storey, R. F. End-Quenching of $TiCl_4$-Catalyzed Quasiliving Polyisobutylene with Alkoxybenzenes for Direct Chain End Functionalization. *Macromolecules* **2010**, *43* (21), 8724−8740.
(53) Morgan, D. L.; Storey, R. F. End-Quenching of Quasi-Living Isobutylene Polymerizations with Alkoxybenzene Compounds. *Macromolecules* **2009**, *42* (18), 6844−6847.
(54) Ummadisetty, S.; Storey, R. F. Quantitative Synthesis of *exo*-Olefin-Terminated Polyisobutylene: Ether Quenching and Evaluation of Various Quenching Methods. *Macromolecules* **2013**, *46* (6), 2049−2059.
(55) Bermeshev, M. V.; Bulgakov, B. A.; Genaev, A. M.; Kostina, J. V.; Bondarenko, G. N.; Finkelshtein, E. Sh. Cationic Polymerization of Norbornene Derivatives in the Presence of Boranes. *Macromolecules* **2014**, *47* (16), 5470−5483.
(56) Slugovc, C.; Demel, S.; Riegler, S.; Hobisch, J.; Stelzer, F. Influence of Functional Groups on Ring Opening Metathesis Polymerisation and Polymer Properties. *J. Mol. Catal. A: Chem.* **2004**, *213* (1), 107−113.
(57) Reactions were carried out in 5/1 (v/v) THF/NMP cosolvent mixture, with NMP used to increase the solubility of the (oxa) norbornene precursors in THF. Additionally, the reaction rate was greatly improved by the addition of an 18-crown-6 phase transfer catalyst.
(58) Le, D.; Montembault, V.; Soutif, J.-C.; Rutnakornpituk, M.; Fontaine, L. Synthesis of Well-Defined ω-Oxanorbornenyl Poly(ethylene oxide) Macromonomers via Click Chemistry and Their Ring-Opening Metathesis Polymerization. *Macromolecules* **2010**, *43* (13), 5611−5617.
(59) The slope of this plot is theoretically equivalent to the exact mass of the isobutylene repeat unit, 56.06 Da. The *y*-intercept is theoretically equivalent to $f \times EG + I + C$, where f is the functionality of the polymer (1 in this study), EG is the exact mass of the (oxa) norborene moiety, I is the exact mass of the TMPCl initiator residue (C_8H_{17}), and C is the exact mass (106.91 Da) of the major isotope of the associated Ag cation.
(60) Storey, R. F.; Curry, C. L.; Brister, L. B. Carbocation Rearrangement in Controlled/Living Isobutylene Polymerization. *Macromolecules* **1998**, *31* (4), 1058−1063.
(61) Dimitrov, P.; Emert, J.; Hua, J.; Keki, S.; Faust, R. Mechanism of Isomerization in the Cationic Polymerization of Isobutylene. *Macromolecules* **2011**, *44* (7), 1831−1840.
(62) Morgan, D. L.; Storey, R. F. Primary Hydroxy-Terminated Polyisobutylene via End-Quenching with a Protected *N*-(ω-Hydroxyalkyl)pyrrole. *Macromolecules* **2010**, *43* (3), 1329−1340.
(63) Villemin, E.; Herent, M.-F.; Marchand-Brynaert, J. Functionalized Phosphonated Half-Cage Molecules as Ligands for Metal Complexes. *Eur. J. Org. Chem.* **2012**, *2012* (31), 6165−6178.
(64) Wang, Y.; Cai, J.; Rauscher, H.; Behm, R. J.; Goedel, W. A. Maleimido-Terminated Self-Assembled Monolayers. *Chem. - Eur. J.* **2005**, *11* (13), 3968−3978.

DOI: 10.1021/acs.macromol.7b01655
Macromolecules 2017, 50, 7458−7467